
a1996001a

DESY 95-229
November 1995

ISSN 0418-9833

Deep Inelastic Scattering

Invited Talk at the International Europhysics Conference

on High Energy Physics, Brussels

27 July - 2 August, 1995

Franz Eisele

Physikalisches Institut der Universität Heidelberg

DEEP INELASTIC SCATTERING

INVITED TALK AT THE INTERNATIONAL EUROPHYSICS CONFERENCE ON HIGH ENERGY PHYSICS, BRUSSELS
27 JULY - 2 AUGUST, 1995

FRANZ EISELE

Physikalisches Institut der Universität Heidelberg, Philosophenweg 12, D 69120 Heidelberg

New experimental results on inclusive structure function measurements as well as on hadronic final states are presented and discussed. Special emphasis is given to the new results from HERA which are relevant for the discussion of QCD dynamics at small parton momentum fractions x.

1 Introduction

Deep inelastic scattering (DIS) is a fundamental process for measuring quark and gluon densities in the nucleon and to make quantitative tests of QCD. The theoretical predictions are very solid based on perturbative QCD and QCD sum rules. DIS is also one of the best processes to measure α_s. The large extension of the kinematic range by the HERA experiments especially the extension to small x has created new challenges as discussed by A. Mueller in his plenary talk[1]. The key question at HERA is the QCD dynamics at small values of the parton momentum fraction x (Bjorken x) in the DIS regime e.g. for values of the four momentum transfer squared $Q^2 > 1\ GeV^2$.

2 New Structure Function Measurements

The new muon collaboration NMC has presented the final analysis of muon proton and muon deuteron data taken back in 1989 at muon energies of 90, 120, 200 and 280 GeV [2]. These data cover the low x range down to $x \approx 8{*}10^{-3}$ starting at $Q^2 = 1\ GeV^2$. Preliminary results have been presented by the Fermilab experiment E665. This experiment has used muon beams on P, D and nuclei with energies in the range $350\ GeV < E_\mu < 600\ GeV$. The experiment has suffered from low integrated luminosities. A special low angle forward spectrometer has allowed them however to provide unique data at very low $Q^2 > 0.3\ GeV^2$ and low x ($10^{-3} < x < .01$) [3] Both muon experiments have also shown measurements of F_2^n/F_2^p and of structure function ratios for heavy targets [4] down to very small x- values.

New preliminary results on F_2^p based on the 1994 data have been presented by the HERA experiments H1 [7] and ZEUS [8] which represent a big step forward. They are based on a total integrated luminosity of about 2.8 pb^{-1} - an increase by a factor 6 compared to published results. This allowed a much better look into the high Q^2 region. At the same time both experiments have also extended the kinematic range significantly towards smaller values of x and Q^2.

The new data from NMC and E665 close very nicely the gap between the well established results of the fixed target experiments BCDMS [9] and SLAC and the HERA measurements such that we have now a good coverage over a huge kinematic range given by

$$0.3\ GeV^2 < Q^2 < 10000\ GeV^2$$

$$5 * 10^{-5} < x < 0.75$$

for the inclusive structure function of the proton. This kinematic range matches also well the range of parton momentum fractions which is probed at the TEVATRON and in future at the LHC in hard scattering processes.

A new measurement of the polarized structure function $g_1^d(x)$ extending down to x values of .003 has been obtained by the SMC collaboration [6,5].

2.1 Measurements at very high Q^2 from HERA

The large increase of integrated luminosity allows a sensitive look into the so far inaccessible region at very high Q^2. Both experiments have accumulated about 0.8 pb^{-1} for e^-p and 2.8 pb^{-1} for e^+p running and 150 charged current events $ep \rightarrow \nu X$. Figure 1 shows the differential cross sections $d\sigma/dQ^2$ for neutral and charged current interaction at high Q^2 compared to standard model expectations [10,11].

The measurements agree well with the standard model. For the first time we are able to see that the charged current cross section indeed becomes comparable to the neutral current cross section for $Q^2 > m_W^2$ as expected. The measurements are sensitive to the

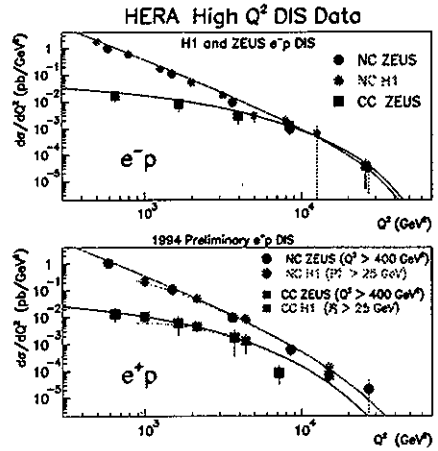

Figure 1: Measurements of Charged Current and Neutral Current cross sections for e^+p and e^-p interactions compared to standard model predictions from the HERA experiments.

propagator mass of the W-boson within an error of $\Delta m_W = \pm 15 GeV$.

The high Q^2 region is also the region where we can sensitively look for signs of new physics. The H1 collaboration has found two events which created a lot of excitement when they were first found [12]. One event is of the type $e^+p \to \mu^+X$ the second one $e^+p \to e^-X$. These are signatures which would occur in several new particle scenarios. Within the standard model both events can hovever be explained by photoproduction of a W-boson which decays semileptonically with probabilities of 3% resp. 10% for the two events (using H1 statistics only).

The relatively high statistics of neutral current events at high Q^2 allows already sensitive searches for compositeness. Both experiments have e.g. reported upper limits on contact interactions with mass scales > 1 to 2 TeV depending on coupling comparable to the results from other colliders [13].

This is clearly only a first glimpse into HERA's future. Much higher luminosity is expected in future.

2.2 *New F_2-measurements from fixed target experiments*

An example of the new structure function measurements of NMC is shown in figure 2 which shows the deuteron structure function F_2^d at small values of x versus Q^2. The data points for the four energies are shown separately. The addition of the 120 and 200 GeV data points gives a better handle on systematic errors and should also allow in the near future to get a measurement of the longitudinal structure function.

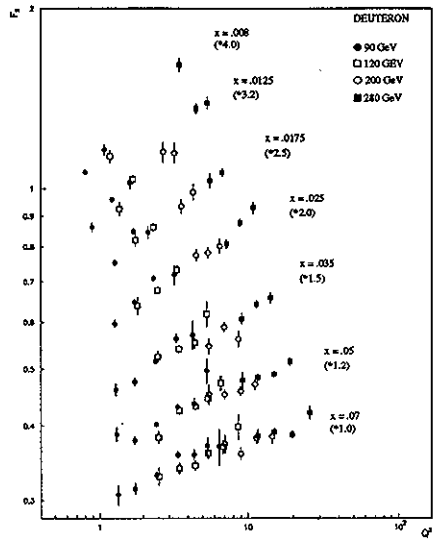

Figure 2: Measurement of F_2^d versus Q^2 for low values of x for the four beam energies (NMC,preliminary).

Figures 3 and 4 show a comparison of the NMC data with the published data of BCDMS [9] and SLAC for F_2^d together with a common QCD NLO fit to all three data sets for protons and deuterons. There is remarkably good agreement also in normalisation which agrees to a level of about 2% , well within the given normalisation errors. The systematic uncertainties of the NMC measurements are shown as dashed error bands and are at a level of 3 to 5 % at small x and 1 to 1.5 % at large x.

Both NMC and E665 have presented preliminary results on the structure function ratio $F_2^n(x)/F_2^p(x)$ down to x values of 10^{-5}.These measurements are systematically very precise because H_2 and D_2 targets have been used simultaneously in the same beam. They provide the basis for an improved measurement of

$$F_2^p - F_2^n = (1 - F_2^n/F_2^p)/(1 + F_2^n/F_2^p) * F_2^d$$

The preliminary result of NMC is shown in figure 5 together with the evaluation of the Gottfried sum rule

$$S_G = \int_0^1 (F_2^p - F_2^n)dx/x = 1/3 + 2/3 \int_0^1 (\bar{u}(x) - \bar{d}(x))dx$$

at the average $Q^2 = 4\ GeV^2$.

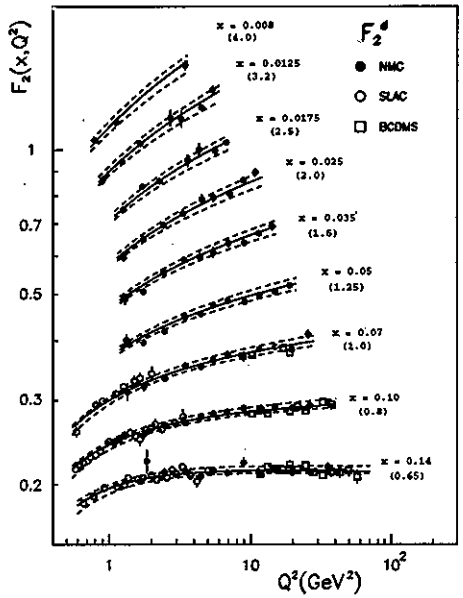

Figure 3: The structure function F_2^d versus Q^2 for low values of x as measured by NMC compared to published results of BCDMS and SLAC.

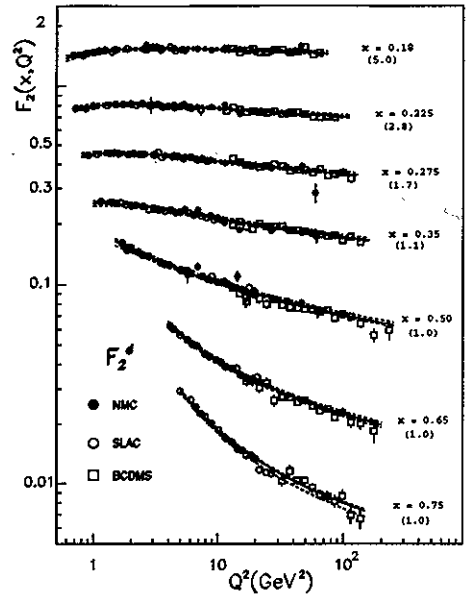

Figure 4: The structure function F_2^d versus Q^2 for high values of x as measured by NMC compared to published results of BCDMS and SLAC.

The experimental result, extrapolated to x=0 using the assumption $F_2^p - F_2^n \sim x^\alpha$ is measured as

$$S_G(exp) = 0.216 \pm .024_{exp} \pm .009_{shad.} \pm .015_{H.Twist}$$

for $Q^2 = 4\ GeV^2$, significantly different from 1/3 as naively expected. The value includes large corrections for shadowing and higher twist contributions which also introduce sizeable error contributions. NMC has also studied the Q^2 dependence of S_G and found no significant change such that the Gottfried sum rule is violated in the Q^2 range from 0.5 GeV^2 to 10 GeV^2. The measurement can be translated into a flavour asymmetry of the sea quarks :

$$\int_0^1 (\bar{u}(x) - \bar{d}(x))dx = -0.176 \pm .043$$

The flavour asymmetry has been confirmed by a more direct measurement of the NA51 Drell-Yan experiment which compared pp and pD production of muon pairs and found [14]

$\bar{u}/\bar{d} = 0.51 \pm .04 \pm .05$ for $x = 0.18$ and $Q^2 = 25\ GeV^2$.

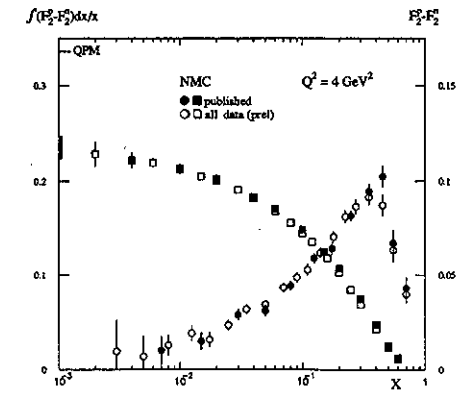

Figure 5: The difference $F_2^p - F_2^n$ and the cumulative integral $S_G(x_{min}$ *to* 0.8) as measured by NMC (prelim.)

The latest results presented at this conference by the muon experiments is something like the last word of

fixed target experiments on unpolarised structure functions (except for the neutrino program at Fermilab which will continue for some more years). Our knowledge on quark distributions and of α_s is based on these experiments especially SLAC(ep) , BCDMS, NMC and the neutrino experiment CCFR and will not be improved in the forseeable future. These experiments have carried out a heroic effort over many years of hard work and they have brought our knowledge to a rather satisfactory status.

2.3 Polarized Structure Functions

The SLAC and NMC spectrometers have been revived for the measurement of polarised structure functions which requires a longitudinally polarised lepton beam and a longitudinally polarised target and the possibility to change their relative polarisation. Muon beams are naturally polarised from pion decay and a polarisation of 80% is easily obtained. SLAC on the other hand has learned how to produce electron beams with high polarisation ($\sim 80\%$). Measurements have so far been obtained from proton deuterium and ^3He targets. The experiments measure the asymmetry

$$A_1(x,Q^2) \sim (d\sigma^{\uparrow\downarrow} - d\sigma^{\uparrow\uparrow})/(d\sigma^{\uparrow\downarrow} + d\sigma^{\uparrow\uparrow})$$

and get from there the spin structure function

$$g_1(x,Q^2) \approx A_1(x) * F_1(x,Q^2) = A_1(x) * F_2(x,Q^2)/x/(1+R)$$

where the asymmetry is so far assumed to be independent of Q^2 and the small contribution of the structure function g_2 is neglected - both approximations are justified at the present level of accuracy. The structure functions can be related in the QPM to the quark densities $q_i^{\uparrow}(x)$ *and* $q_i^{\downarrow}(x)$ for finding a quark of flavour i with spin parallel resp. antiparallel to the nucleon spin by:

$$F_1(x) = \frac{1}{2}\sum_i e_i^2 (q_i^{\uparrow}(x) + q_i^{\downarrow}(x))$$

$$g_1(x) = \frac{1}{2}\sum_i e_i^2 (q_i^{\uparrow}(x) - q_i^{\downarrow}(x)) = \frac{1}{2}\sum_i e_i^2 \Delta q_i(x)$$

Finally the spin fraction carried by flavour i can be obtained by

$$\Delta q_i = \int_0^1 \Delta q_i(x) dx$$

The spin muon collaboration SMC [5,6] has presented a new measurement of $A_1^d(x)$ as shown in figure 6 together with the measurements of the SLAC E143 experiment [15].

The SMC result covers the range $0.003 \leq x \leq 0.7$ and $1 \leq Q^2 \leq 60\ GeV^2$ whereas the SLAC data starts only at x = 0.03 and is at lower Q^2

The corresponding measurements of $g_1^d(x)$ *and* $g_1^n(x)$ are shown in figure 7.

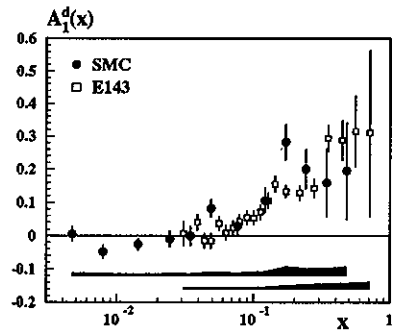

Figure 6: Deuteron asymmetry as measured by SMC and E143.

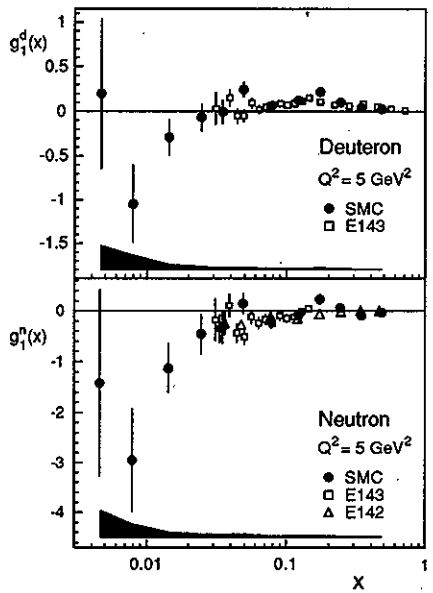

Figure 7: Polarised structure functions g_1^d and g_1^n as evaluated by SMC and the SLAC experiments E142 and E143.

The most surprising result of the new SMC measurement is the negative value of g_1^d at small x. This also reflects in large negative values of $g_1^n(x)$ at small x which was directly measured by experiment E142 on He^3 and was derived by a comparison of D and p measurements by

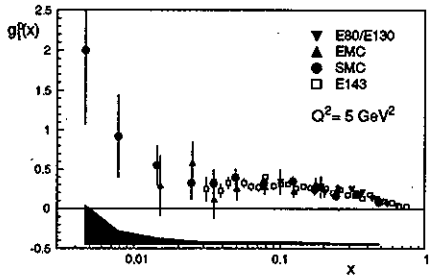

Figure 8: Polarised structure function g_1^p as evaluated by SMC and E143.

E143 and SMC (figure 7). Since also g_1^n shows indication of a nontrivial x- dependence at small x this has raised serious discussions on the small x behaviour of polarised structure functions and on how to extrapolate them to x=0 as required for the QCD sum rules. This will be discussed further in section 4.

2.4 New Measurements of F_2^{ep} at HERA

Both HERA experiments have presented new structure function measurements based on the data taken in '94[8,7]. Figure 9 shows the distribution of DIS events recorded in '94 by H1 in the log x - log Q^2 plane.

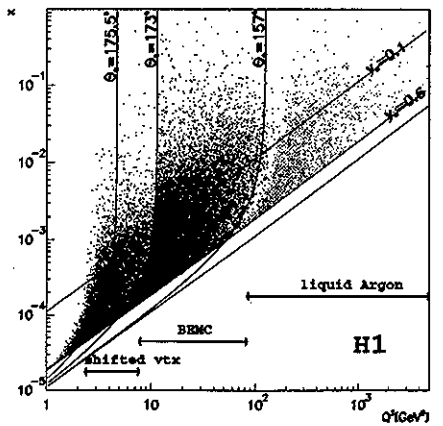

Figure 9: Distribution of the '94 DIS events from H1 in the plane x- Q^2.

Whereas the '93 data was restricted to electron scattering angles of $< 173°$, the kinematic range in '94 has been extended by both H1 and ZEUS towards small Q^2 and x by taking a small fraction of data (58 pb^{-1}) with the interaction vertex shifted by 62 cm. H1 has already analysed the full '94 data set whereas the preliminary ZEUS analysis is so far restricted to the low Q^2 shifted vertex data and data points at very high Q^2. In addition H1 has evaluated a subsample of events where the initial electron has lost energy by radiation, thus reducing the CM energy in the hard collision. This extends the useful range down to $Q^2 = 1\ GeV^2$. The Q^2 dependence of F_2 for fixed values of x is shown in figure 10 for the new HERA measurements compared to the fixed target measurements.

It can be noted that the H1 and ZEUS measurements are in good agreement with each other and that they match well with the fixed target measurements. There is good agreement in normalisation within the systematic error bands of the NMC data. The preliminary H1 data points are dominated by systematic errors for $Q^2 < 500\ GeV^2$ which are typically $\delta F_2/F_2 \approx 10\%$. Major error contributions come from the electron and hadron energy calibrations of 1.5 % resp. 5% which translate into errors of F_2 of up to 7 % resp. 5 %. It will be possible to reduce these errors in future. The normalisation error for the new data is about 1.5%.

The x dependence of the same measurements for bins in Q^2 is shown in figure 11.

It can be noted that F_2 changes in the HERA range by more than a factor two as a function of x for nearly all bins in Q^2.

3 QCD Interpretation and Parton Distributions

3.1 Gluon and Quark Distributions

It's well known, that the Q^2 evolution of the published DIS structure function measurements including the HERA '93 data can be well described by the 'standard' next to leading order (NLO) DGLAP evolution equations [16]. This is still true for the preliminary '94 data as shown by the H1 collaboration which has fitted their new measurements together with the latest NMC and BCDMS measurements of F_2^{ep} for $Q^2 > 4\ GeV^2$. The fit involves 11 shape parameters and 6 relative normalisations [19]. The result is shown in figure 12 and is obviously able to describe the x and Q^2 dependence down to the smallest values of Q^2. It also underlines the large rise of F_2 with Q^2 at small x. This rise is strongly coupled to the gluon distribution and can therefore be used to determine it assuming the validity of the DGLAP evolution equation in this kinematic range. This has been published both by ZEUS and H1 [20,21] based on the 93 data and is shown in figure 13 including the estimate of systematic uncertainties which are clearly dominant. Also shown are the gluon distributions as given by some

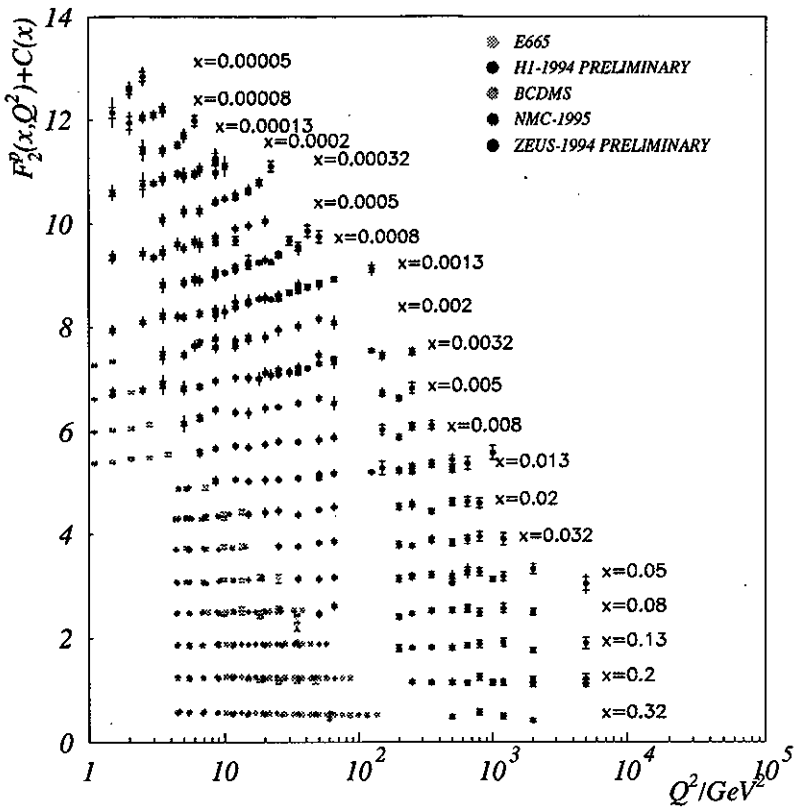

Figure 10: Measurements of F_2^p vs. Q^2 for different x from HERA and from fixed target experiments.

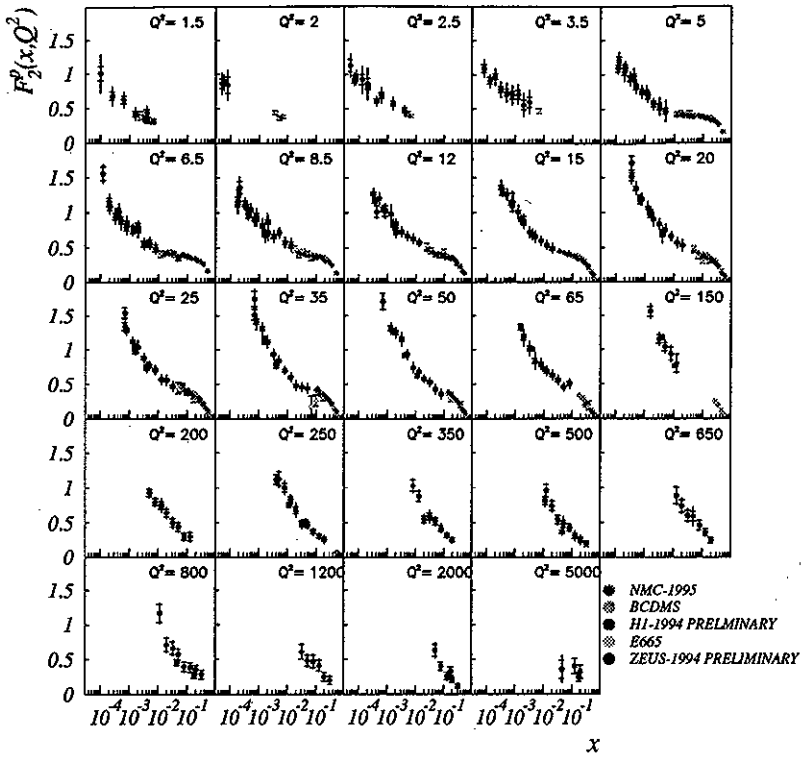

Figure 11: Measurements of F_2^p vs. x for different Q^2 from HERA and from fixed target experiments.

of the global fits to all DIS data - see below. Whereas these parametrisations - except for MSR(D_0') which is prior to HERA - clearly agree with the determinations of H1 and ZEUS they give not the slightest idea how well we actually know this distribution. As a result the gluon distribution in the proton is now reasonably well constrained down to $x \sim 3 * 10^{-4}$. Gluons rise steeply at small x - typically $xG(x,Q^2) \sim x^{-\lambda_g}$ with $\lambda_g \approx .25$ to 0.4 and are about 20 times more abundant at small x compared to sea quarks.

The transfer of the universal parton distributions from DIS to other hard scattering processes in e.g. $\bar{p}p$ collisions requires a complete and consistent set of parton distributions which are obtained by the global analysis of selected DIS data and a few measurements of hard processes in hadron hadron collisions . The procedure for global fits is as follows:

- choose selected, consistent experimental data sets.
- choose a parametrisation for all parton distributions at $\mu^2 = Q_0^2$. This requires between 15 and 25 parameters.
- use NLO DGLAP evolution to evolve these input distributions to the Q^2 values of the data points and compare.

Where does our present knowledge of parton distributions come from?

Shortly, the quark distributions and α_s are determined by BCDMS and the CCFR DIS experiments. The gluon distribution is determined by NMC and HERA data plus a constraint for large x from prompt photon production in pp collisions. The newest sets of parametrisations also use constraints on the flavour asymmetries u/d and $\bar{u}/\bar{d}$ from hadron hadron collisions which however are always restricted to a small x-range. For a recent review see e.g. [23].

There are three major sets of parametrisations which are at a comparable level of sophistication. Two of them, MRS (Martin, Roberts and Stirling) [24] and CTEQ [25] chose a value of $Q_0^2 = 4\ GeV^2$ and use only data above that starting point. Another approach is used by GRV (Gück, Reya and Vogt) [26] which start at very low $Q_0^2 = 0.34\ GeV^2$ and make no explicit use of HERA data. Since this approach is both successful and instructive its worth while to have a closer look to it.

The original idea of GRV is to start with only valence distributions of the 'constituent quarks' and to create all gluons and sea quarks by the DGLAP evolution. This concept did not work, they have to parametrise also gluon and sea quark distributions at Q_0^2 but these are assumed to be valence like e.g. they are zero at x=0 as shown in figure 14. The NLO DGLAP evolution equations are used to evolve them to higher Q^2 as shown e.g . in figure 15 where a large rise of the gluon distribution and of the sea quarks and hence also F_2 is necessarily predicted. This approach was the only one which necessarily predicted the steep rise of F_2 at small x as observed at HERA. It equally well predicts that the slopes in x have to decrease towards low Q^2 as actually observed in

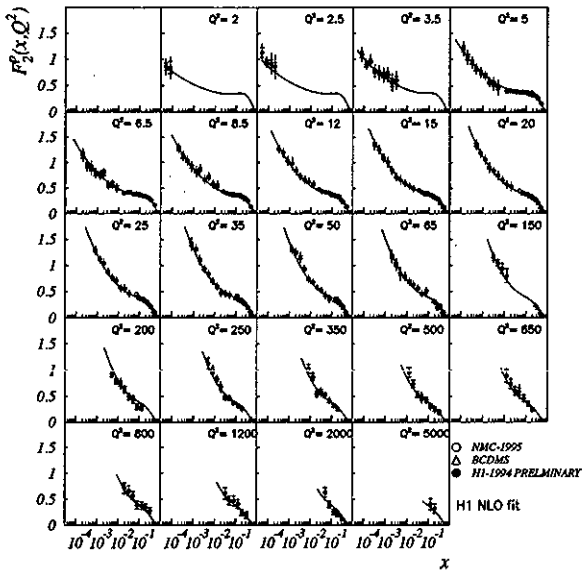

Figure 12: H1 '94 measurement of F_2^p vs. Q^2 for fixed values of x, compared to a NLO QCD fit which includes also the NMC and BCDMS data.

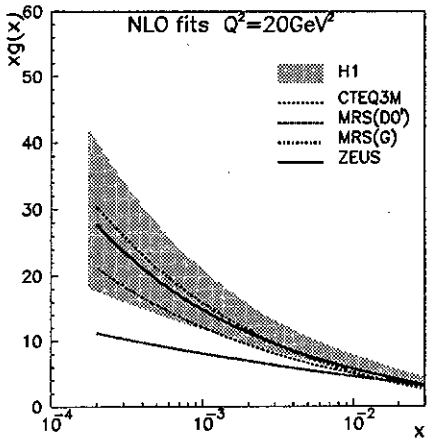

Figure 13: Determination of the gluon distribution from NLO QCD fits by H1 and ZEUS [20,21] compared to some global parametrisations. The H1 result shows the error band incl. systematic errors, ZEUS has a similar error band.

the new HERA data.

The predictions of several parton parametrisation are compared to the new '94 data at small Q^2 in figure 16. The top row shows the Q^2 bins below 4 GeV^2 with the predictions of GRV94 [26] and Regge inspired models [27] which both have a definite prediction for the x-dependence. Whereas the Regge models are unable to describe the observed x-dependence in the HERA range, GRV94 does very well. The bottom row shows the higher Q^2 bins where also recent MRS and CTEQ parametrisations are shown. They will certainly be able to improve the present sets - it would be desirable however to extend them to lower values of Q^2. Of specific interest as pointed out by A. Mueller [1] is the information if GRV is able to also describe the evolution down to even smaller values of Q^2. The answer can be seen in figure 17 which shows the preliminary data from experiment E665 extending down to $Q^2 = 0.5\ GeV^2$. This data is also well described by the Regge model of Donnachie and Landshoff [27] based on the soft pomeron idea but equally well by GRV94.

The interest in GRV is thus not the specific assumptions about the parton distributions at small Q^2 but the undeniable fact, that the use of ordinary DGLAP evolution which sums only the $\ln Q^2$ and $\ln Q^2 * \ln(1/x)$ terms neglecting all $\ln(1/x)$ terms is able to describe the evolution of F_2 in x and Q^2 over this large range at small x. It has been shown by Lipatov and collaborators [17] that neglection of the $\ln(1/Q^2)$ terms but keeping the $\ln(1/x)$ terms - an approximation which should be good at sufficiently low x for all Q^2 - gives a very different evolution equation (BFKL-equation). Specifically the gluon distribution is expected in this approximation to behave as $xG(x,Q^2) \sim x^{-\lambda_g}$ for x→0 , with $\lambda_g \approx 0.5$ ('Lipa-

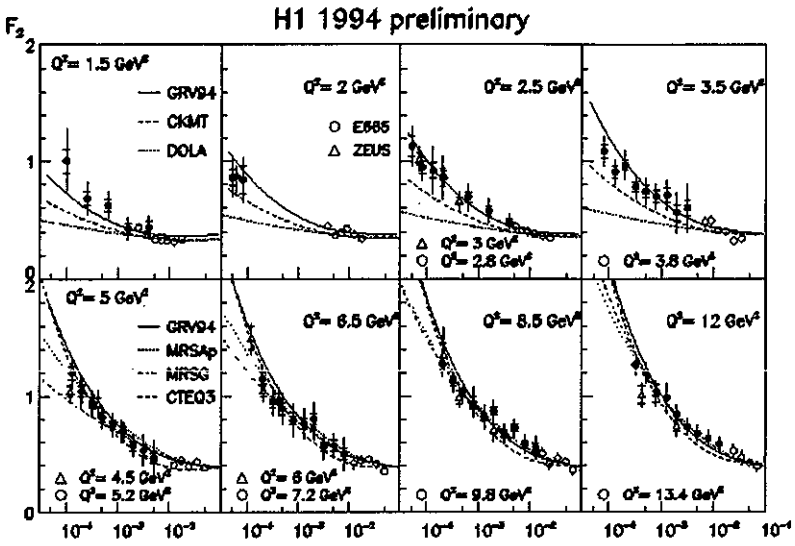

Figure 16: Measurements of F_2^p vs. x for different low Q^2 bins from HERA and from experiment E665 compared to different parton parametrisations. (DOLA and CKMT: Regge inspired parametrisations, MRSx,CTEQ3:global DGLAP fits.)

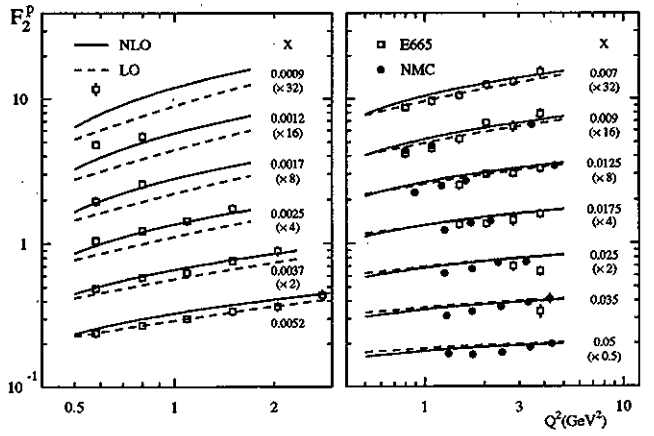

Figure 17: GRV parametrisation compared to low Q^2 data of E665 and NMC.

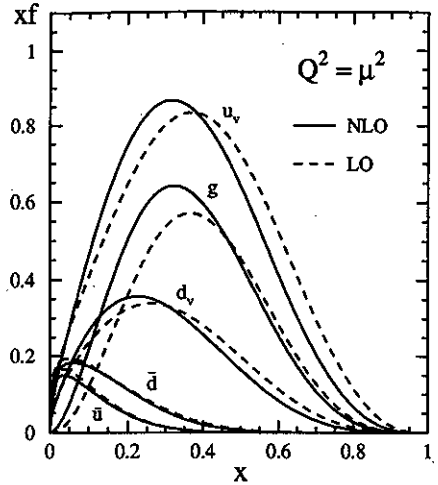

Figure 14: Input distribution for the GRV94 parametrisation at $Q_0^2 = 0.34\ GeV^2$.

tov Pomeron' or 'hard Pomeron'). The success of GRV demonstrates that the interpretation of the steep rise of F_2 at low x does not need this Lipatov behaviour but that NLO DGLAP evolution does it all alone and is moreover able to bridge naturally the transition from the 'soft pomeron' to the 'hard pomeron' regime as discussed by Levy [28]. Why do we see no sign of the $\ln(1/x)$ terms which can give very sizable effects at a given order as has been demonstrated by several groups [18]?

3.2 Testing QCD dynamics at small x

The use of rather involved numerical QCD fits to the data is not too illuminating. We can ask ourselves if there is a more sensitive way to see possible deviations from the DGLAP evolution at small x. The answer is yes. The success of the GRV approach suggests that the HERA data may be near to the 'asymptotic' double log solution of the DGLAP equations. If we define the double log variables

$$\sigma = \sqrt{ln(x_0/x) * ln(t/t_0)} = \sqrt{ln(x_0/x) * ln(\alpha_s(Q_0^2)/\alpha_s(Q^2))}$$

$$\rho = \sqrt{ln(x_0/x)/ln(t/t_0)} \qquad t = ln(Q^2/\Lambda^2)$$

then for ***sufficiently*** large t and small x the QCD evolution becomes much simpler and the shape of F_2 at small x is actually predicted because it is determined by radiation processes independent of the starting distribution.

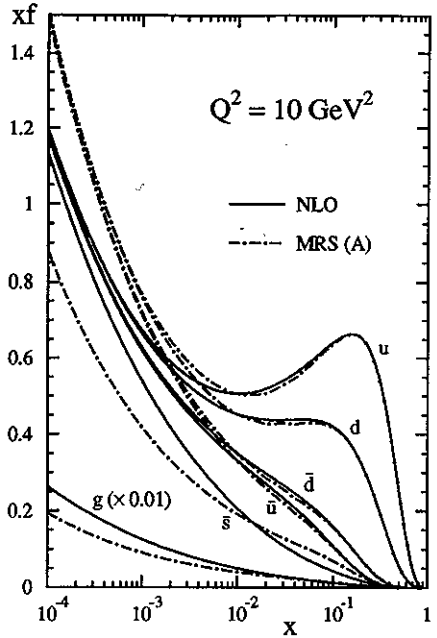

Figure 15: GRV94 parton densities after evolution to Q^2=10 GeV^2.

This fact can be expressed by two scaling relations which should hold in the asymptotic region as shown by Georgi and Politzer in '74 [29] and recently revived by Ball and Forte [30].

$$ln(R_F'(\sigma,\rho) * F_2(\sigma,\rho)) = a + 2\gamma * \sigma$$

$$R_F(\sigma,\rho) * F_2(\sigma,\rho) = f(\gamma/\rho) * a' \rightarrow const$$

Here R_F' *and* R_F are known functions as defined e.g. in reference [30], $2\gamma = 4\sqrt{3/(11-2/3n_f)} = 2.4$ is predicted by QCD and $f(\gamma/\rho)$ is a smooth function which depends on the boundary conditions for the gluon distribution at (x_0, t_0) and should got to 1 for large ρ.

The use of double log scaling variables thus eliminates the leading 'universal' scaling violations ; we should therefore be more sensitive to other contributions. There is of course no prediction what Q^2 sufficiently large means - this has to be answered by experiment. It has also to be pointed out that the scaling relations will only hold IF the gluon distribution is nonsingular at the boundaries. It has been demonstrated convincingly by Ball and Forte [30] that a 'Lipatov type' behaviour $xG(x_0,t_0) \sim x^{-\lambda_g}$ at (x_0,t_0) with $\lambda_g \sim .4$ would spoil double log scaling drastically.

Double log scaling was shown by the H1 collaboration in 93 to hold approximately for $Q^2 > 4.5\ GeV^2$ [21]. The new data is displayed in figure 18 for a value of $Q_0^2 = 1.0\ GeV^2$, where data for Q^2 below and above 5 GeV^2 are shown with different symbols.

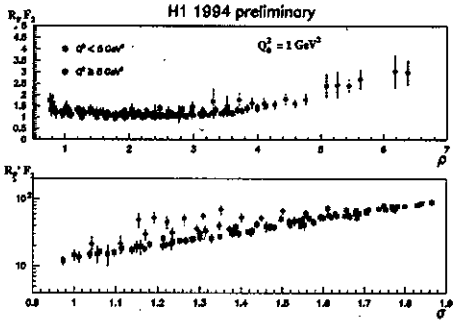

Figure 18: Test of double log scaling with the '94 H1 data using $Q_0^2 = 1\ GeV^2$. Low and high Q^2 points are shown separately.

Double log scaling requires that $log(R_F' * F_2)$ is linear in σ with slope 2γ for all points whereas $R_F * F_2$ becomes constant for sufficiently large ρ. Whereas the high Q^2 data shows excellent double log scaling, the data at low Q^2 shows systematic deviations from it. They rise at high values of ρ and deviate systematically from the straight line in σ. Deviations of this kind can be due to higher order corrections or subleading terms in the DGLAP description or indicate signs of unusual QCD dynamics. As a first attempt H1 has tried to minimize higher order corrections by a better choice of Q_0^2. Indeed a choice of $Q_0^2 = 0.5\ GeV^2$ leads to approximate double log scaling over the whole Q^2 range as shown in figure 19.

A better way of doing the tests would be to confront the data with the calculated NLO corrections and to see if they describe the observed deviations (this work is in progress). We may nevertheless conclude that double log scaling starting at rather low values of Q^2 is a dominant feature of the H1 data on F_2 leaving little room for BFKL [17] like contributions.

A quantitative analysis gives a value of $(2\gamma)_{exp} = 2.5 \pm 0.03 \pm .10_{syst}$ for a value of $\Lambda_{LO} = 250\ MeV$ in good agreement with the LO QCD expectation of 2.4. It should be pointed out that the observation of double log scaling is only possible if α_s shows very strong running with Q^2 as can be seen from the definition of σ. In the H1 range $ln(x_0/x)$ varies by a factor 2.5 which means that $ln(\alpha_s)$ has to vary by the same amount. The slope

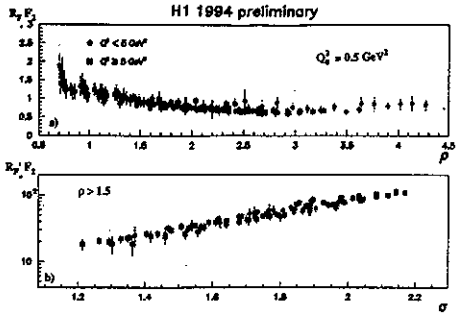

Figure 19: Test of double log scaling for $Q_0^2 = 0.5\ GeV^2$.

in σ is therefore highly sensitive to the value of A.

To summarise this part we can say:

- very surprisingly the Q^2 evolution of F_2 shows a very simple behaviour at small x over the whole kinematic range of the new HERA data.
- It is hard to beleive that the observation of double log scaling even at low Q^2 is accidential since 2γ is measured correctly which is a non trivial QCD test.
- the linearity in σ depends critically on A.

So we have to ask: are we already in the asymptotic regime? We can hope that the observation of double log scaling could be used for a precise and sensitive test of the Q^2 evolution of α_s and a precise determination of A. An analysis along this line has actually been published by Ball and Forte [31] using published 93 data of H1 and ZEUS. They have made a NLO analysis of this data with the following results: 1) double log scaling is preserved in NLO. 2) NLO corrections improve agreement with data. 3) a fit to the data with only 4 free parameters : Q_0, λ_g, λ_q, *and* $\alpha_s(m_Z)$, where λ_g *and* λ_q define the low x behaviour of gluons and quarks at Q_0^2, they find

$$\alpha_s(m_Z) = 0.120 \pm .005 \pm .009\ (theory).$$

This result is encouraging. The problem is that their analysis is dependent on the expansion scheme. Their approach is criticised by other theorists so we have to wait for further clarification.

It will be very interesting to see which conclusions theorists will draw from the success of GRV and the observation of double log scaling at low Q^2. This is a real surprise and the first reaction of experts at this conference was that they have no explanation and need rethinking.

3.3 summary of QCD tests at low x

The results discussed so far can be summarised as follows:

- there is no evidence yet for new log(1/x) components in the QCD evolution of structure functions. They must however exist in some (x,Q^2) range.
- the DGLAP evolution works remarkably well down to Q^2 as low as 0.5 GeV^2 and $x \sim 5{*}10^{-5}$ as shown by the success of GRV and the observation of double log scaling.
- HERA measurements of F_2 have dramatically improved since last year. They still wait for serious confrontation with theory.
- Further extensions of the kinematic range down to $Q^2 \approx .5\ GeV^2$ and improvements in precision are already reached with the data recorded by the HERA experiments in '95.
- there is some hope that the low x data can be used for quantitative QCD tests and precision measurements of α_s.

4 QCD Sum Rules

4.1 Fundamental QCD Sum Rules

The fundamental sum rules contain only nonsinglet contributions. They test very basic and fundamental QCD predictions and can also be used to make precision measurements of α_s.

The Gross -Llewellyn-Smith sum rule:
This sum rule is well known: It gives the definite QCD prediction that the integral over the valence quark densities in the Bjorken limit $Q^2 \rightarrow \infty$ has to be exactly 3. The QCD corrections are known to third order [32] up to uncertainties due to higher twist contributions for which only an estimate exists (ΔHT):
$\int_0^1 xF_3^{NS}(x,Q^2)dx/x =$
$3{*}\{1-\alpha_s/\pi - a(n_f)(\alpha_s/\pi)^2 - b(n_f)(\alpha_s/\pi)^3{+}\} - \Delta HT$
This sum rule can be tested in neutrino experiments.

The Bjorken Sum Rule:
This sum rule depends on the spin densities of the proton and neutron:
$\int_0^1 x(g_1^p - g_1^n)dx/x =$
$\frac{1}{6}\ g_A{*}\{1-\alpha_s/\pi - 3.5833(\alpha_s/\pi)^2 - 20.2153(\alpha_s/\pi)^3$
$-(\sim 130)(\alpha_s/\pi)^4 + ...\} - C_{HT}/Q^2$
In the Bjorken limit the integral has to be exactly 1/6 of the axial coupling constant as measured in neutron beta decay [32].

$SU(3)_f$ sum rule:
In principle there is a third sum rule based on SU(3) flavour symmetry, for which however there is no direct experimental test. Its validity will be *assumed* in the following.

$\Delta u + \Delta d - 2\Delta s = g_8 {*} C_{NS}(Q^2)$
where g_8 can be measured via hyperon semileptonic decays.

4.2 Sum Rules involving flavour singlet contributions

There are no firm QCD predictions for these sum rules because the evolution of the singlet contributions involves anomalous dimensions. Here we are concerned with two sum rules:

- The Gottfried sum rule discussed in section 2, which gave the surprising result , that the momentum fraction carried by $\bar{u}$ is smaller than the momentum fraction carried by $\bar{d}$.
- The Ellis-Jaffe Sum Rule related to the spin densities in the nucleon, which will be discussed below.

These singlet sum rules are those which provided the *surprises* . They give important information about the constituent quarks.

A common feature of all sum rules is that they involve the integral over quark densities down to x = 0. Since every experiment can only measure down to a lowest value x_{min} if $Q^2 > 1\ GeV^2$ is required, every evaluation of a sum rule involves some model dependent extrapolation to x=o.

4.3 New measurements of the Gross-Llewellyn-Smith sum rule

The CCFR neutrino collaboration has presented to this conference a new evaluation in bins of Q^2 between $1 \leq Q^2 \leq 20\ GeV^2$. In order to do that they combined their own data with low energy data from bubble chambers [33]. The sum rule is well satisfied including the higher order QCD corrections and tested to the level of about 10% . They can also use the measured Q^2 dependence to determine $\alpha_s(Q^2)$. They find:

$$\alpha_s(3\ GeV^2) = 0.26^{+.02}_{-.03}(stat.)\pm.02(syst)\pm.03(highertwist)$$

corresponding to a value

$$\alpha_s(m_Z) = 0.108^{+.003}_{-.005}(stat) \pm .004(syst.)^{+.005}_{-.006}(HT)$$

This is a precision measurement of α_s at a small scale. It suffers however from rather large uncertainties due to higher twist corrections.

4.4 Sum Rules involving Moments of spin structure functions

We have to determine the moments of the polarised structure functions $\Gamma_1 = \int_0^1 g_1(x,Q^2)dx$. This poses several problems:
1) The data has to be evolved to a common value of Q^2, whereas different x- values cover a Q^2 range of $1 < Q^2 < 6.5\ GeV^2$ for experiment E143 and $1 < Q^2 < 60\ GeV^2$ for SMC. This extrapolation is done assuming that the asymmetry A(x) is independent of Q^2 which is not strictly true but an acceptable approximation given the large experimental errors.
2) The integrals have to be extrapolated to x=1 which is uncritical and safe.
3) The integral has to be extrapolated to x=0. This poses major problems and gives rise to large uncertainties.

The case is best illustrated by a discussion of Γ_1^n. The present knowledge of $g_1^n(x)$ is summarised in figure 7 which shows both the direct measurement of E142 which stops at x=.03 and the evaluations of SMC and E143 by a combination of their proton and deuteron measurements. The SMC data extend down to x=.003 ,their x points below the SLAC data show strong negative values. If we take this result serious - and there is no reason why we should not - then the contribution to Γ_1^n for $.003 < x < .03$ is equally large as the rest of the integral for x> 0.3. The SLAC experiments have set g_1^n constant for x < .03 , grossly underestimating the contribution to the sum rule or at least of the uncertainty involved in this extrapolation. The published values of the integrals are therefore inconsistent and cannot be averaged.

A much better way to combine the data sets has recently be done by the SMC collaboration [15]. They average the SLAC and SMC measurements of the asymmetries, interpolate to a common value $Q^2 = 5\ GeV^2$, and then form the integral keeping of course the low x SMC points. The extrapolation from x=.003 to x=0 is done assuming a functional behaviour $g_1(x) \sim x^\alpha$ with $0 < \alpha < 0.5$. This gives new 'world averages':

$$\Gamma_1^p = .136 \pm .010 \qquad \Gamma_1^n = -.067 \pm .016 \qquad Q^2 = 5\ GeV^2$$

The value of Γ_1^n differs by a factor three from the published E142 result!. Using these moments we can now test the sum rules.

Test of the Bjorken sum rule

This test is graphically shown in figure 20.

Numerically one gets
$\Gamma_1^p - \Gamma_1^n = 0.203 \pm .023$ *for* $Q^2 = 5\ GeV^2$
to be compared to the QCD prediction
$(\Gamma_1^p - \Gamma_1^n)_{QCD} = 0.185 \pm .004$
for a value of $\alpha_s(m_Z) = .117 \pm .005$. In summary the Bjorken sum rule is tested to an accuracy of about 10%. Unfortunately the data is not good enough to use this sum rule for a quantitative determination of α_s mainly because Γ_1^n has too large uncertainties.

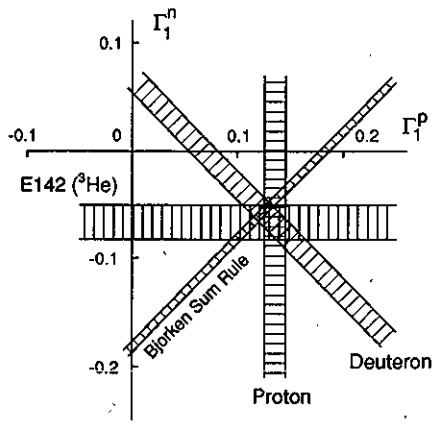

Figure 20: World averaged experimental results and Bjorken prediction for the first moments Γ_1^p *and* Γ_1^n at $Q^2 = 5\ GeV^2$ [15].

Evaluation of the Ellis-Jaffe Sum Rule

The proton and neutron moments can be expressed as follows:
$\Gamma_1^{p,n} = (\pm\frac{1}{12}g_A + \frac{1}{36}g_8) {*} C_{NS}(Q^2)$
$+\frac{1}{9}\Delta\Sigma(Q^2) {*} C_{SI}(Q^2)$

$$\Delta\Sigma(\infty) = \Delta u + \Delta d + \Delta s - n_f\frac{\alpha_s}{2\pi}\Delta G$$

where ΔG is the moment of the polarized gluon distribution and the Q^2 dependent corrections are given by QCD. From the last expression it can be seen that $\Delta\Sigma(\infty)$ is *not only* the spin fraction carried by the quarks, in addition it contains a term coming from the density of polarised gluons which enters by the axial anomaly. The origin of the famous 'spin crises' is based here: Ellis and Jaffe assumed that ΔG *and* Δs are zero as expected in the constituent quark model.

The experimental measurements of the moments can now be used to determine a best value for $\Delta\Sigma(\infty)$. The global SMC analysis gives

$$\Delta\Sigma(\infty) = .19 \pm .07$$

fixing:

$$g_A = 1.2573 \pm .0028 \quad and \quad g_8 = 0.579 \pm .016$$

This value is much smaller than the Ellis-Jaffe prediction of $\Delta\Sigma = g_8 = 0.58$. Since there are only two measurements but three unknown contributions to the moments we have to make model assumptions:
1) we can assume ΔG=0. In this case we find $\Delta s =$

$-0.13 \pm .03$. Published results of this most common approach are summarised in figure 21.

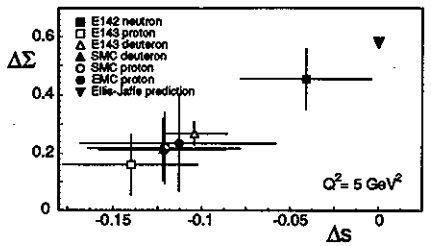

Figure 21: Experimental results on the total ($\Delta\Sigma$) and strange (Δs) quark contributions to the nucleon spin at $Q^2 = 5\ GeV^2$.

All points cluster in one area far from the Ellis-Jaffe point except the old published point of E142. This point however moves to the other points if the extrapolation to x=0 is done according to the new SMC data as explained above.
2) We can assume $\Delta s = 0.0$ and fix $\Delta\Sigma_q = \Delta u + \Delta d = g_8 = .58$ to the Ellis-Jaffe value. In this case we find $\Delta G = 3.2 \pm .75$. Such a large value of ΔG would restore the prediction of the constituent quark model.

new experimental input

The situation can mainly be improved by new experimental input. A very promising road is to disentangle the various contributions to the moments like valence, sea quark and gluon contributions. The new HERMES experiment at HERA , which just started data taking, will be able to disentangle quark distributions (valence ,sea quarks, up, down and eventually strange quarks) by measuring semiinclusive asymmetries of pions and kaons like

$$A^{\pi^+} = \frac{N_\uparrow^{\pi^+} - N_\downarrow^{\pi^+}}{N_\uparrow^{\pi^+} + N_\downarrow^{\pi^+}}$$

A new proposal (HMC=heavy muon collaboration) is pending at CERN SPS to determine ΔG via charm production in polarised muon nucleon scattering. Such an experiment could answer the question if the axial anomaly is responsible for the smallness of $\Delta\Sigma$.
The problem of the low x region could be attacked at HERA by storing polarised protons in the proton ring. This is technically feasible and would allow to measure spin structure functions down to values of $x = 10^{-5}$.

Experimental efforts along these lines are very interesting because they can bridge the gap between current quarks and constituent quarks.

4.5 summary on QCD sum rules

- The *sacred* sum rules , the Bjorken and Gross-Llewellyn-Smith sum rules, are verified to a level of about 10%. They have the potential to determine α_s very precisely because they are measured at low scales. They suffer however from higher twist corrections and from uncertainties of extrapolations to x=0.

- The sea is not flavour symmetric. We find $\bar{d} > \bar{u} > \bar{s}$ from the Gottfried sum rule and direct measurements in Drell Yan processes.

- The spin structure of the nucleon is complicated. The simple picture suggested by the success of the constitutent quark model does not work, because we are testing the parton structure inside the constituent quarks, and this seems to be complicated.

5 Deep Inelastic Final States at HERA

The HERA collider experiments measure the complete hadronic final state apart from the particles disappearing in the beam pipe. Compared to e^+e^- colliders HERA has the advantage that it offers a huge scale variation within one experiment. If we take Q as the relevant scale, which it is in the Breit frame, then the range $1 < Q < 40 GeV$ can be used now which can be extended to 100 GeV with increasing luminosity. HERA is thus ideally suited to measure 1/Q corrections.
Compared to LEP we start with one strongly interacting parton in the initial state which makes life more difficult but also more interesting. Thus HERA is an intermediate step from LEP to the hadron colliders.

New results presented to this conference included interesting results on single particle spectra [34] which will not be discussed here.

5.1 Multijet events at HERA

Multijet events are expected at HERA as a consequence of higher order QCD processes. In next to leading order events with two hard partons in the final state are predicted via the the photon gluon fusion process $g\gamma \rightarrow \bar{q}q$ and the QCD Compton process $q\gamma \rightarrow qg$. Both processes are proportional to $\alpha_s(Q^2)$, the gluon fusion process requires in addition the knowledge of the gluon distribution in the proton. Ideally one would like to make a simultaneous analysis over the full Q^2 range with $\alpha_s(Q^2)$ and $xg(x,Q^2)$ to be determined. Such an analysis is under way but is theoretically and technically demanding. So far the analysis has been broken up in two steps:

Determination of $\alpha_s(Q^2)$ for $Q^2 > 100\ GeV^2$

In this kinematic range ($x > 0.01$) the photon gluon fusion process makes only a modest contribution. Preliminary analyses of the '94 data have been presented by both H1 and ZEUS [35]. They avoid the target fragmentation region and the higher order effects of initial state gluon radiation by requiring $\Theta_{jet} > 10^o$ (H1) and $z_p = P * p_{jet}/P * q > 0.1$ (H1 and ZEUS) and use a modified JADE algorithm with the separation parameter $y_c = m_{ij}^2/W^2$. The 2-jet fraction

$$R_{2+1}(Q^2, y_c) = \sigma_{2+1}(Q^2, y_c)/\sigma(Q^2)$$

is then compared to NLO QCD calculations [36] and $\alpha_s$determined in bins of Q^2. Here the +1 stands for the proton spectator jet. The H1 and ZEUS results are shown in figure 22.

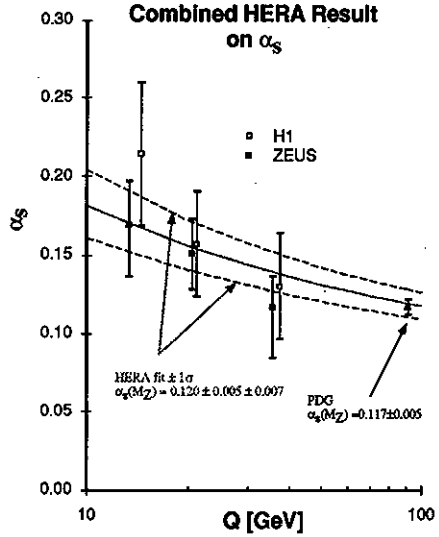

Figure 22: Measurements of $\alpha_s$by H1 and ZEUS from the 2-jet rate at high Q^2 compared to the world average.

The lines show the combined HERA result (central value and $\pm 1\ \sigma$) together with the present world average for $\alpha_s(M_Z)$. The numerical value is:

$$\alpha_s(m_Z) = 0.120 \pm .005 \pm .007(syst)$$

This result is competitive with the corresponding LEP measurement from the three jet rate and is presently systematically limited by calibration errors and scale dependences. This will be improved in the next round.

Direct determination of the gluon distribution at low x

The 2-jet sample for $Q^2 < 80\ GeV^2$ and $.0003 < x_{Bj} < .0015$ is dominated by the photon gluon contribution which gives about 75% of all events. It has therefore been used by H1 [38] to determine directly the gluon distribution in leading order (LO) using a fixed value for α_s(LO). The analysis uses a cone algorithm with cone width $\Delta R = 1$ and asks for a transverse momentum in the γp CM system of $p_T^* > 3.5$ GeV. A total of 328 (2+1) jet events have been found by H1 in '93 which cover the range $.002 < x_g < .2$. The result of this first direct measurement of the gluon distribution at small x is shown as solid points in figure 23 compared to indirect deter-

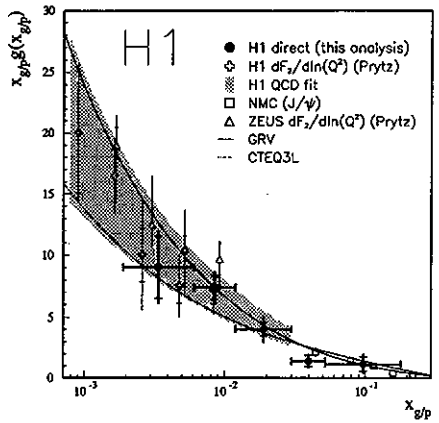

Figure 23: $xG(x,Q^2)$ evaluated in LO. The solid points give the direct measurement from the 2-jet rate at smallx , other results of H1 and ZEUS from the analysis of scaling violations are shown for comparison.

minations from the scaling violations of F_2 at small x as determined by H1 and ZEUS in leading order. There is overall good consistency .

5.2 Transverse energy flow at small x

The study of transverse energy flow especially at mid rapidity between the current quark and the proton direction is another very promising handle to study QCD dynamics at small x as will be shown in the following.

Rather surprising results have been obtained by H1 [39] which studied the transverse energy flow $dE_T/d\eta^*$ in the γp CM system both for photoproduction ($Q^2 \approx 0.$) and for DIS scattering as a function of Q^2. This is shown in figure 24. One surprising result is that the transverse energy per unit of rapidity at mid rapidity ($-.5 < \eta < .5$)

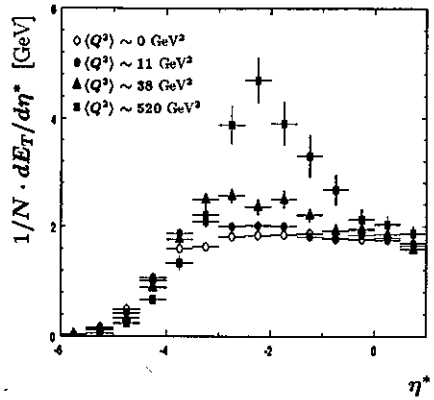

Figure 24: Transverse energy versus rapidity in the γp CM system as measured by H1 for photoproduction and DIS in different bins of Q^2.

is about 2 GeV nearly independent of Q^2. It is especially surprising that photoproduction and high Q^2 events have the same mid rapidity energy flow not only in average but also in the differential E_T distribution. This result can be qualitatively summarised by saying that the memory of large virtuality at the γ-vertex is lost very fast over a distance $\Delta\eta \approx 1.5$. The other surprising fact is that in the current region (the region of the scattered quark) the transverse energy flow changes very slowly from Q^2=0.0 up to $Q^2 \approx 11\ GeV^2$. It is therefore no surprise that none of the presently available Monte Carlo generators is able to describe the transverse energy flow at small x.

The E_T flow in e-p interactions can also be compared with that of $\pi - p$ and p-p interactions. The surprising result is that the transverse energy flow at mid rapidity is universal independent of projectile and target for the same invariant mass of the hadronic system. This gives some hope that DIS scattering can be a handle to resolve this question because definite QCD predictions can be made for the transverse energy flow at high Q^2.

The diagram which is relevant for the calculation of the transverse energy flow is shown in figure 25. This diagram is calculable in QCD. However , not surprisingly, such a calculation faces the same problems at small x as the analysis of scaling violations. Again we are faced with contributions proportional to $ln(1/Q^2), \{ln(1/Q^2\}^n * \{ln(1/x)\}^m$ and $\ln(1/x)$ which cannot be dealt with simultaneously. Neglection of the $\ln(1/x)$ terms leads to the DGLAP predictions. In this case parton emission along the ladder is strongly ordered in k_T, the jet production and the transverse energy at mid rapidity are therefore small. In contrast neglection

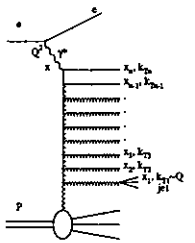

Figure 25: Ladder diagram to describe the transverse energy flow in DIS .

of the $\ln(1/Q^2)$ terms leads to the BFKL predictions with no k_T ordering giving enhanced E_T flow and large jet rate which moreover is predicted to rise towards small x. The study of transverse energy flow at mid rapidity gives therefore another handle on QCD dynamics at small x which is more direct and more discriminative than the study of scaling violations of F_2.

Measurements of the transverse energy flow in DIS at small x .

The transverse energy flow for DIS events at small x has been systematically studied by both H1 and ZEUS [40] using their calorimeters and compared to the DGLAP and BFKL predictions at the parton level. In addition they also compare to 'standard' DIS Monte Carlos. One of their results is shown in figure 26. It can be seen that the transverse energy flow is large and badly described by the present version of a DGLAP MC with LUND fragmentation (MEPS [42]). Better agreement is reached by using the colour dipole model (CDM) for fragmentation which includes independent particle emission from colour dipoles without k_T ordering, thus simulating a BFKL type of behaviour [41].The predictions of DGLAP and BFKL at the parton level differ very substantially by something like 1 GeV per unit of rapidity - the large value of E_T may therefore be the first indication of unusual (BFKL type) QCD evolution at small x. Unfortunately however, as can be seen from figure 26 the hadronisation process has a very large effect on the energy flow such that the correlation between parton and particle flow is weak. It is therefore unlikely that definite conclusions on the underlying parton dynamics can be drawn from these measurements.

Forward jets at low x. It looks much more promising to measure 'parton' cross sections which can be predicted directly. This is possible using a proposal of A. Mueller [43] which asks for a low x event with an additional jet at large $x_{jet} >> x$ and $k_T^2(jet) \approx Q^2$. For this kinematic selection BFKL predicts a much larger dijet rate than DGLAP.

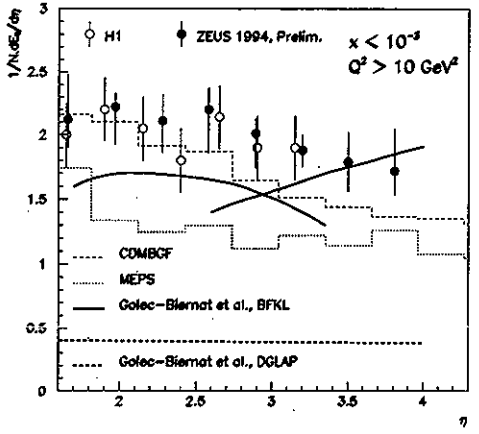

Figure 26: Average transverse energy at mid rapidity as measured by H1 and ZEUS (prel.) at small x compared to QCD predictions at the parton level and predictions of the MEPS and CDM Monte Carlo simulations.

A preliminary analysis along these lines has been published by the H1 collaboration [40] using their '93 data. They clearly show that this measurement is feasible. Based on a total of 429 selected events for $x < 2 * 10^{-3}$ they draw the following conclusions: the 2-jet rate for forward jets is rather high - much higher than the prediction of a DGLAP MC like MEPS. The 2-jet rate increases with 1/x as expected from BFKL contributions. A direct comparison with a BFKL prediction is however not yet possible. We have therefore to wait for future calculations to see if k_T-ordered scenarios are indeed disfavoured. The new '94 data will already allow much more quantitative tests and BFKL calculations are under way such that there is a good chance that the study of final states will give much better clarification of QCD dynamics at low x.

6 Hadronic Final State in Rapidity Gap Events

Rapidity gap events have been discussed in detail in his plenary talk by A. Levy [28]. He also defines the relevant variables and structure functions. Here I want to add information concerning the hadronic final state which will also help to understand these events further.

Rapidity gap events which show no energy flow at mid rapidity have the following global properties [44,45].

- the fraction of rapidity gap events is about 10% independent of x and Q^2
- the single paticle spectra for these events are identical to ordinary DIS events if we compare them at $W^2 = M_x^2$.
- the fraction of K^0 is the same as in ordinary DIS events.
- We see a large fraction of single jet and dijet events ($\sim 35\%$ at $M_x = 35\ GeV$) (see figure 27).
- the fraction of dijet events with rapidity gap at small x is 8 ± 2 % of the "$\gamma - g$ sample" used for the direct measurement of the gluon distribution.

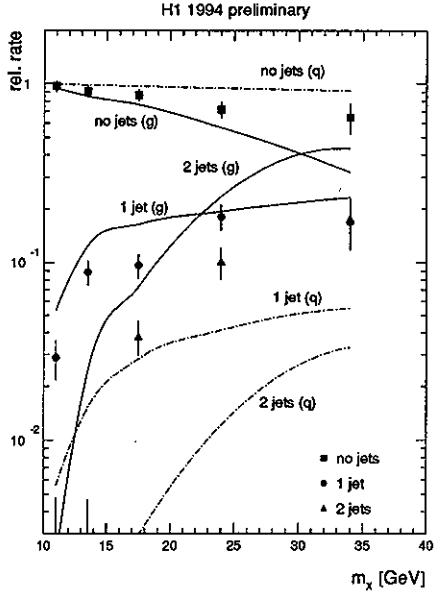

Figure 27: Fraction of multijet events vs. hadronic mass m_x for rapidity gap events as evaluated by H1. The analysis looks for jets with $E_T > 5\ GeV$ in a cone of radius 1 in the $\gamma^* - p$ rest system.

The observation of jets and the constant ratio of rapidity gap events independent of x and Q^2 clearly demonstrate that we are faced with a hard scattering process.

A. Levy has discussed in detail the success of the 'Pomeron model' of Ingelmann and Schlein to describe the rapidity gap events. In this model the process is described as the emission of a quasireal Pomeron from the proton with flux $\sim 1/x_P$ followed by the deep inelastic

scattering of the electron from a parton in the Pomeron. We can ask however if this is the only possible description. It is certainly surprising that rapidity gap events look so similar to ordinary DIS events:
Rapidity gap events look - at the present level of accuracy - like ordinary DIS events with reduced invariant hadronic mass $W^2 = M_x^2$. They occur at a constant level of about 10%. They can therefore be successfully described by the assumption that they are standard DIS events with unusual fragmentation.

A very interesting model using this idea has been proposed by Buchmüller and Hebbeker [46]. This model is much more economic than the 'Pomeron' model because it predicts the rate and the differential cross section for the rapidity gap events. The model describes the rapidity gap events as deep inelastic scattering from gluons via the γg fusion process, the standard diagram for scattering from sea quarks at low x. The $q\bar{q}$ pair is produced in a coloured state. The basic assumption of the model is that there is a fast statistical colour rotation in the field of the nucleon which leads to a colour neutralisation ot the pair in 1/9 of all cases. In this model the variable x_P is the momentum fraction of the gluon whereas the 'Pomeron structure function' is given by the splitting function g$\rightarrow$ $q\bar{q}$. A specific prediction of the model is :

$$F_2^d(x, Q^2, x_P) \approx 0.04 * \frac{1}{x_P} F_2(x_P, Q^2)$$

This prediction is compared to the H1 measurement in figure 28.

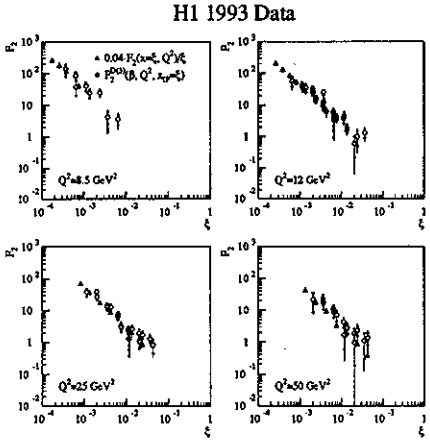

Figure 28: A comparison of the diffractive structure function of H1 to the prediction of the model of Buchmüller [46]

The agreement is quite impressive. To some extent the Buchmueller model is equivalent to a Pomeron model where the pomeron is composed of one hard gluon which carries all its momentum and a soft gluon used for colour neutralisation.

7 Global Summary

Deep inelastic scattering is again a very active research area with two main branches: HERA physics and polarised structure function measurements. The HERA experiments study the QCD dynamics at small x. They study the nature of 'diffraction' and of the 'Pomeron' which so far were not understood in the framework of QCD. They can measure jets and hadronisation properties with large scale variations of $3 < Q^2 < 120\ GeV^2$.

The program on polarised structure functions by SMC, SLAC, HERMES and may be new experiments has the goal to bridge the gap between current quarks and constituent quarks.

DIS experiments have had the major impact on our knowledge of parton distributions in the nucleon. Since HERA we know the gluon distribution rather well down to x-values of $x \approx 10^{-4}$. The steep rise of this distribution towards small x has a significant impact on LHC physics. DIS events have also given some of the most precise measurements of α_s(see e.g. [37]).

The HERA experiments have provided us with a few surprises already which still wait for a satisfactory explanation and further experimental input:

- the observation of the steep rise of F_2 towards low x.
- the observation of double log scaling down to very low values of Q^2.
- the observation of 'universality' of the transverse energy flow at mid rapidity.
- rapidity gap events with surprising properties.

We can be sure that more surprises will be found in the next round.

Acknowledgements

It is a pleasure for me to thank all my colleagues from the different experiments for providing me with their data and for many useful discussions. I thank specially A. Brüll, J. Feltesse, A. Levy, A. Mueller, A. deRoeck, H. Schellmann, U. Straumann and G. Voss for helpful conversations to clarify many points.

1. A. Mueller, plenary talk at this conference, to appear in the proceedings.
2. A. Bruell, NMC coll., to appear in the proceedings, NMC coll., EPS-0648.
3. H. Schellmann, private communication.
4. T. J. Carrol, E665 coll., EPS-0125; A. Witzmann, NMC coll., these proceedings.
5. D. Adams et al., SMC coll., CERN-PPE/95-97.
6. G. Mallot, SMC coll., these proceedings.
7. S. Aid et al., H1 coll., DESY 95-193 and EPS-0470; U. Straumann, to appear in these proceedings.
8. M. Derrik et al., ZEUS coll., DESY 95-193 and EPS-0392; F. Chlebana, ZEUS coll., to appear in these proceedings.
9. A.C. Benvenuti et al.,*Phys. Lett.* **B195** (1987) 97.
10. S.Aid et al., H1 coll., *Phys. Lett.* **B335** (1995) 578.
11. M. Derrik et al., ZEUS coll., DESY 95-053 and EPS-0376.
12. T. Ahmed et al.,H1 coll., DESY 95-248 and EPS-0786.
13. S.Aid et al., H1 coll., *Phys. Lett.* **B353** (1995) 578.
14. A. Baldit et al., *Phys. Lett.* **B332** (1994) 244.
15. For a recent summary see R. Voss,"Experiments on Polarised Deep Inelastic Scattering", proceedings of the Workshop on Deep Inelastic Scattering and QCD, Paris, April 1995.
16. Yu.L. Dokshitzer, Sov. Phys. JRTP **46** (1977) 641. ; V. N. Gribov and L. N. Lipatov, Sov. J. Nucl. Phys. **15** (1972) 438 and 675; G. Altarelli and G. Parisi, *Nucl. Phys.* **28** (1977) 297.
17. E. A. Kuraev, L. N. Lipatov and V. S. Fadin, Sov. Phys. JETP **45** (1977) 199; Y. Y. Balitsky and L. N. Lipatov, Sov. J. Nucl. Phys. **28** (1978) 822
18. F. Hautmann, contribution to this conference, to appear in the proceedings.
19. S.Aid et al., H1 coll., EPS-0471
20. M. Derrik et al., ZEUS coll., *Phys. Lett.* **B345** (1995) 576.
21. T. Ahmed et al., H1 Coll.,*Phys. Lett.* **B354** (1995) 494.
22. G. Parente and A.V. Kotikov, EPS-0126,these proceedings.
23. W. J. Stirling, Proc. Workshop on Deep Inelastic Scattering, Paris, april 1995.
24. A. Martin, R. Roberts, J. Stirling, *Phys. Rev.* **D50** (1994) 6734.and RAL-94-055.
25. J. Botts et al., CTEQ coll., *Phys. Lett.* **B304** (199) 159.
26. M. Glück, E. Reya, A. Vogt, DESY 94-206.
27. A. Donnachie and P.V. Landshoff, *Nucl. Phys.* **B244** (1984) 322.
28. A. Levy, plenary talk at this conference, these proceedings.
29. H. Georgi and H.D. Politzer, *Phys. Rev.* **D9** (1974) 416.
30. R.D. Ball and S. Forte, *Phys. Lett.* **B335** (1994) 77.
31. R. Ball and S. Forte, CERN-TH/95-148.
32. S.A. Larin and J.A.M. Vermaseren, *Phys. Lett.* **B259** (1991) 345.
33. D.A. Harris et al., CCFR coll., EPS-0043. See also W.C. Leung et al.,*Phys. Lett.* **B317** (1993) 655.
34. M. Derrik et al., ZEUS coll., DESY 95-007;S.Aid et al., H1 coll., *Nucl. Phys.* **B445** (1995) 195;M. Derrik et al., ZEUS coll., EPS-0394.and EPS0395; S.Aid et al., H1 coll., EPS-0483.
35. M. Derrik et al., ZEUS coll., DESY 95-182, S.Aid et al., H1 coll., EPS-0396.
36. D. Graudenz, *Phys. Rev.* **D49** (1994) 3291.
37. S. Bethge, 'Summary of α_s Measurements', PITHA-94/30.
38. S.Aid et al., H1 coll., *Nucl. Phys.* **B449** (1995) 3.
39. S.Aid et al., H1 coll., EPS-0480.
40. S.Aid et al., H1 coll., *Phys. Lett.* **B356** (1995) 118;.M. Derrik et al., ZEUS coll., EPS-0391.
41. L. Lönnblad, Comp. Phys. Comm. **71** (1992)15.
42. G. Ingelmann, Proc. of the workshop on Physics at HERA, Hamburg 1991, eds. W. Buchmüller and G. Ingelmann, vol. 3,p. 1366.
43. A. H. Mueller, Nucl. Phys. B (Proc. Suppl.) 18C (1990) 125; J. Phys. G17 (1991) 1443.
44. S.Aid et al., H1 coll., *Phys. Lett.* **B348** (1995) 681;.EPS-0491; EPS-0494.
45. M. Derrik et al., ZEUS coll., DESY 95-093 and EPS-0393.
46. W. Buchmüller and A. Hebbecker, DESY 95-077.